

# ODE Transformer: An Ordinary Differential Equation-Inspired Model for Neural Machine Translation

Bei Li<sup>1</sup>, Quan Du<sup>1,2</sup>, Tao Zhou<sup>1</sup>, Shuhan Zhou<sup>1</sup>, Xin Zeng<sup>1</sup>, Tong Xiao<sup>1,2\*</sup>, and Jingbo Zhu<sup>1,2</sup>

<sup>1</sup>NLP Lab, School of Computer Science and Engineering,  
Northeastern University, Shenyang, China

<sup>2</sup>NiuTrans Research, Shenyang, China

{libei\_neu, duquanneu, zhoutao\_neu, zsh\_neu, iszengxin}@outlook.com  
{xiaotong, zhujingbo}@mail.neu.edu.cn

## Abstract

It has been found that residual networks are an Euler discretization of solutions to Ordinary Differential Equations (ODEs). In this paper, we explore a deeper relationship between Transformer and numerical methods of ODEs. We show that a residual block of layers in Transformer can be described as a higher-order solution to ODEs. This leads us to design a new architecture (call it ODE Transformer) analogous to the Runge-Kutta method that is well motivated in ODEs. As a natural extension to Transformer, ODE Transformer is easy to implement and parameter efficient. Our experiments on three WMT tasks demonstrate the genericity of this model, and large improvements in performance over several strong baselines. It achieves 30.76 and 44.11 BLEU scores on the WMT'14 En-De and En-Fr test data. This sets a new state-of-the-art on the WMT'14 En-Fr task.

## 1 Introduction

Residual networks have been used with a great success as a standard method of easing information flow in multi-layer neural models (He et al., 2016; Vaswani et al., 2017). Given an input  $y_t$ , models of this kind define the output of a layer at depth  $t$  to be:

$$y_{t+1} = y_t + F(y_t, \theta_t) \quad (1)$$

where  $F(\cdot, \cdot)$  is the function of the layer and  $\theta_t$  is its parameter. Interestingly, recent work in machine learning (Weinan, 2017; Lu et al., 2018; Haber et al., 2018; Chang et al., 2018; Ruthotto and Haber, 2019) points out that Eq. (1) is an Euler discretization of the Ordinary Differential Equation (ODE), like this:

$$\frac{dy(t)}{dt} = F(y(t), \theta(t)) \quad (2)$$

where  $y(t)$  and  $\theta(t)$  are continuous with respect to  $t$ . In this way, we can call Eq. (1) an *ODE block*. This finding offers a new way of explaining residual networks in the view of numerical algorithms. Then, one can think of a multi-layer network as applying the Euler method (i.e., Eq. (1)) to solve Eq. (2) subject to the initial conditions  $y(0) = y_0$  and  $\theta(0) = \theta_0$ .

The solution of Eq. (2) has a sufficiently low error bound (call it a *stable solution*) only if  $\theta(t)$  changes slow along  $t$  (Haber and Ruthotto, 2017; Chen et al., 2018). But this assumption does not always hold for state-of-the-art natural language processing (NLP) systems, in which models are non-linear and over-parameterized. For example, language modeling and machine translation systems learn quite different parameters for different layers, especially when the layers are close to the model input (Vaswani et al., 2017; Dai et al., 2019). Also, truncation errors are nonnegligible for the Euler method because it is a first-order approximation to the true solution (He et al., 2019). These problems make the situation worse, when more layers are stacked and errors are propagated through the neural network. It might explain why recent Machine Translation (MT) systems cannot benefit from extremely deep models (Wang et al., 2019; Liu et al., 2020; Wei et al., 2020; Li et al., 2020).

In this paper we continue the line of research on the ODE-inspired method. The basic idea is to use a high-order method for more accurate numerical solutions to the ODE. This leads to a larger ODE block that generates a sequence of intermediate approximations to the solution. We find that the larger ODE block is sufficient to take the role of several ODE blocks with first-order solutions. The benefit

\*Corresponding author.

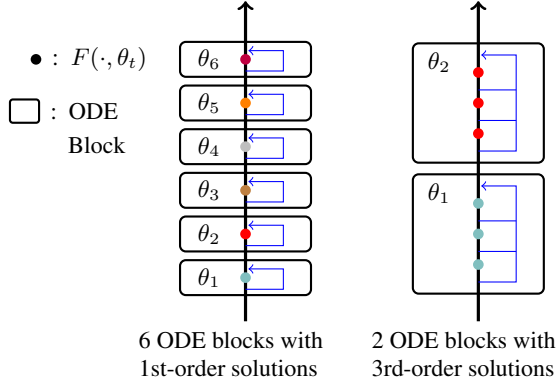


Figure 1: Models with different ODE blocks.

is obvious: the use of fewer ODE blocks lowers the risk of introducing errors in block switching, and the high-order method reduces the approximation error in each ODE block. See Figure 1 for a comparison of different models.

Our method is parameter-efficient because  $\theta(t)$  is re-used within the same ODE block. As another “bonus”, the model can be improved by learning coefficients of different intermediate approximations in a block. We evaluate our method in strong Transformer systems, covering both the wide (and big) model and the deep model. It achieves 30.76 and 44.11 BLEU scores on the WMT14 En-De and En-Fr test sets. This result sets a new state-of-the-art on the WMT14 En-Fr task.

## 2 Transformer and ODEs

We start with a description of Transformer, followed by its relationship with ODEs. We choose Transformer for our discussion and experiments because it is one of the state-of-the-art models in recent MT evaluations.

### 2.1 Transformer

Transformer is an example of the encoder-decoder paradigm (Vaswani et al., 2017). The encoder is a stack of identical layers. Each layer consists of a self-attention block and a feedforward network (FFN) block. Both of them equip with a residual connection and a layer normalization unit. Note that the term “block” is used in many different ways. In this paper, the term refers to any neural network that is enhanced by the residual connection (occasionally call it a *residual block*).

Following the Pre-norm architecture (Wang et al., 2019), we define a block as

$$y_{t+1} = y_t + G(\text{LN}(y_t), \theta_t) \quad (3)$$

where  $\text{LN}(\cdot)$  is the layer normalization function<sup>1</sup>, and  $G(\cdot)$  is either the self-attention or feedforward network. The decoder shares a similar architecture, having an additional encoder-decoder attention block sandwiched between the self-attention and FFN blocks.

### 2.2 Ordinary Differential Equations

An ordinary differential equation is an equation involving a function  $y(t)$  of a variable  $t$  and its derivatives. A simple form of ODE is an equation that defines the first-order derivative of  $y(t)$ , like this

$$\frac{dy(t)}{dt} = f(y(t), t) \quad (4)$$

where  $f(y(t), t)$  defines a time-dependent vector field if we know its value at all points of  $y$  and all instants of time  $t$ . Eq. (4) covers a broad range of problems, in that the change of a variable is determined by its current value and a time variable  $t$ .

This formulation also works with Pre-norm Transformer blocks. For notational simplicity, we re-define  $G(\text{LN}(y_t), \theta_t)$  as a new function  $F(y_t, \theta_t)$ :

$$F(y_t, \theta_t) = G(\text{LN}(y_t), \theta_t) \quad (5)$$

We then relax  $y_t$  and  $\theta_t$  to continuous functions  $y(t)$  and  $\theta(t)$ , and rewrite Eq. (3) to be:

$$y(t + \Delta t) = y(t) + \Delta t \cdot F(y(t), \theta(t)) \quad (6)$$

where  $\Delta t$  is the change of  $t$ , and is general called *step size*. Obviously, we have  $\Delta t = 1$  in Transformer. But we can adjust step size  $\Delta t$  using a limit, and have

$$\lim_{\Delta t \rightarrow 0} \frac{y(t + \Delta t) - y(t)}{\Delta t} = F(y(t), \theta(t)) \quad (7)$$

Given the fact that  $\lim_{\Delta t \rightarrow 0} \frac{y(t + \Delta t) - y(t)}{\Delta t} = \frac{dy(t)}{dt}$ , Eq. (7) is an instance of Eq. (4). The only

<sup>1</sup>We drop the parameter of  $\text{LN}(\cdot)$  for simplicity.

difference lies in that we introduce  $\theta(t)$  into the right-hand side of Eq. (4).

Then, we say that a Pre-norm Transformer block describes an ODE. It has been found that Eq. (3) shares the same form as the Euler method of solving the ODE described in Eq. (7) (Haber and Ruthotto, 2017). This establishes a relationship between Transformer and ODEs, in that, given  $F(\cdot, \cdot)$  and learned parameters  $\{\theta_t\}$ , the forward pass of a multi-block Transformer is a process of running the Euler method for several steps.

### 3 The ODE Transformer

In numerical methods of ODEs, we want to ensure the precise solutions to the ODEs in a minimum number of computation steps. But the Euler method is not “precise” because it is a first-order method, and naturally with local truncation errors. The global error might be larger if we run it for a number of times<sup>2</sup>. This is obviously the case for Transformer, especially when the multi-layer neural network arises a higher risk of instability in solving the ODEs (Haber and Ruthotto, 2017).

#### 3.1 High-Order ODE Solvers

Here we use the Runge-Kutta methods for a higher order solution to ODEs (Runge, 1895; Kutta, 1901; Butcher, 1996; Ascher and Petzold, 1998). They are a classic family of iterative methods with different orders of precision<sup>3</sup>. More formally, the explicit Runge-Kutta methods of an  $n$ -step solution is defined to be:

$$y_{t+1} = y_t + \sum_{i=1}^n \gamma_i F_i \quad (8)$$

$$F_1 = hf(y_t, t) \quad (9)$$

$$F_i = hf(y_t + \sum_{j=1}^{i-1} \beta_{ij} F_j, t + \alpha_i h) \quad (10)$$

where  $h$  is the step size and could be simply 1 in most cases.  $F_i$  is an intermediate approximation to the solution at step  $t + \alpha_i h$ .  $\alpha$ ,  $\beta$  and  $\gamma$  are coefficients which can be determined by the Taylor series of  $y_{t+1}$  (Butcher, 1963). Eq. (10) describes a

<sup>2</sup>The global error is what we would ordinarily call the error: the difference between  $y(t)$  and the true solution. The local error is the error introduced in a single step: the difference between  $y(t)$  and the solution obtained by assuming that  $y(t-1)$  is the true solution

<sup>3</sup>A  $p$ -order numerical method means that the global truncation error is proportional to  $p$  power of the step size.

sequence of solution approximations  $\{F_1, \dots, F_n\}$  over  $n$  steps  $\{t + \alpha_1 h, \dots, t + \alpha_n h\}$ . These approximations are then interpolated to form the final solution, as in Eq. (8).

The Runge-Kutta methods are straightforwardly applicable to the design of a Transformer block. All we need is to replace the function  $f$  (see Eq. (10)) with the function  $F$  (see Eq. (5)). The advantage is that the function  $F$  is re-used in a block. Also, the model parameter  $\theta_t$  can be shared within the block<sup>4</sup>. In this way, one can omit  $t + \alpha_i h$  in Eq. (10), and compute  $F_i$  by

$$F_i = F(y_t + \sum_{j=1}^{i-1} \beta_{ij} F_j, \theta_t) \quad (11)$$

This makes the system more parameter-efficient. As would be shown in our experiments, the high-order Runge-Kutta methods can learn strong NMT systems with significantly smaller models.

The Runge-Kutta methods are general. For example, the Euler method is a first-order instance of them. For a second-order Runge-Kutta (RK2) block, we have

$$y_{t+1} = y_t + \frac{1}{2}(F_1 + F_2) \quad (12)$$

$$F_1 = F(y_t, \theta_t) \quad (13)$$

$$F_2 = F(y_t + F_1, \theta_t) \quad (14)$$

This is also known as the improved Euler method. Likewise, we can define a fourth-order Runge-Kutta (RK4) block to be:

$$y_{t+1} = y_t + \frac{1}{6}(F_1 + 2F_2 + 2F_3 + F_4) \quad (15)$$

$$F_1 = F(y_t, \theta_t) \quad (16)$$

$$F_2 = F(y_t + \frac{1}{2}F_1, \theta_t) \quad (17)$$

$$F_3 = F(y_t + \frac{1}{2}F_2, \theta_t) \quad (18)$$

$$F_4 = F(y_t + F_3, \theta_t) \quad (19)$$

See Figure 2 for a comparison of different Runge-Kutta blocks. It should be noted that the method presented here can be interpreted from

<sup>4</sup>Although we could distinguish the parameters at different steps in a block, we found that it did not help and made the model difficult to learn.

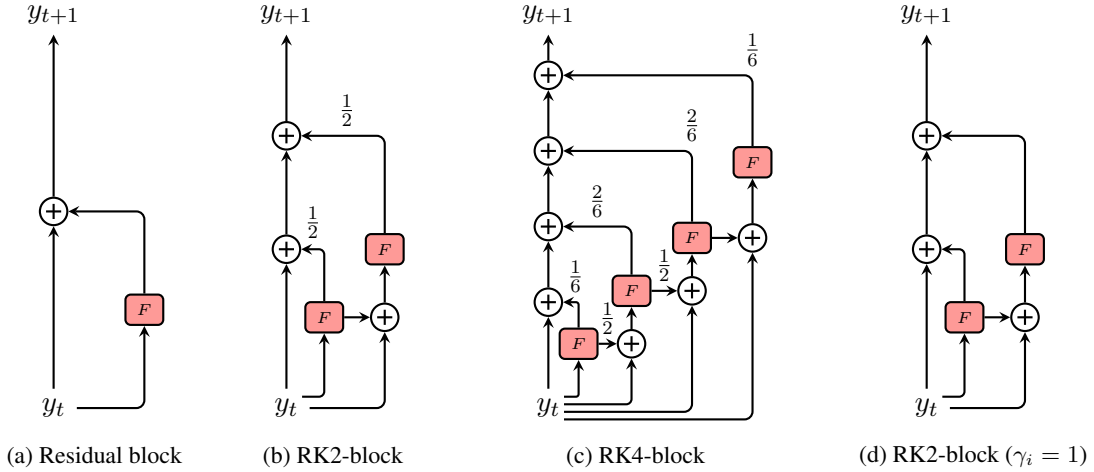


Figure 2: Architectures of ODE Transformer blocks.

the perspective of representation refinement (Greff et al., 2017). It provides a way for a function to update the function itself. For example, Universal Transformer refines the representation of the input sequence using the same function and the same parameters in a block-wise manner (Dehghani et al., 2019). Here we show that inner block refinements can be modeled with a good theoretical support.

### 3.2 Coefficient Learning

In our preliminary experiments, the RK2 and RK4 methods yielded promising BLEU improvements when the model was shallow. But it was found that the improvement did not persist for deeper models. To figure out why this happened, let us review the Runge-Kutta methods from the angle of training. Take the RK2 method as an example. We rewrite Eq. (12) by substituting  $F_1$  and  $F_2$ , as follow

$$y_{t+1} = y_t + \frac{1}{2}F(y_t, \theta_t) + \frac{1}{2}F(y_t + F(y_t, \theta_t), \theta_t) \quad (20)$$

Let  $\mathcal{E}$  be the loss of training,  $L$  be the number blocks of the model, and  $y_L$  be the model output. The gradient of  $\mathcal{E}$  at  $y_t$  is

$$\frac{\partial \mathcal{E}}{\partial y_t} = \frac{\partial \mathcal{E}}{\partial y_L} \cdot \frac{1}{2^{L-t}} \cdot \prod_{k=t}^{L-1} (1 + g_k) \quad (21)$$

where

$$g_k = \left(1 + \frac{\partial F(y_k, \theta_k)}{\partial y_k}\right) \cdot \left(1 + \frac{\partial F(y_k + F(y_k, \theta_k), \theta_k)}{\partial y_k + F(y_k, \theta_k)}\right) \quad (22)$$

Seen from Eq. (29),  $\frac{\partial \mathcal{E}}{\partial y_t}$  is proportional to the factor  $\frac{1}{2^{L-t}}$ . This leads to a higher risk of gradient vanishing when  $L$  is larger.

The problem somehow attributes to the small coefficients of  $F_i$ , that is,  $\gamma_1 = \gamma_2 = \frac{1}{2}$ . A natural idea is to empirically set  $\gamma_i = 1$  to eliminate the product factor of less than 1 in gradient computation, although this is not theoretically grounded in standard Runge-Kutta methods. We rewrite Eq. (20) with the new coefficients, as follows

$$y_{t+1} = y_t + F(y_t, \theta_t) + F(y_t + F(y_t, \theta_t), \theta_t) \quad (23)$$

Then, we have the gradient, like this

$$\frac{\partial \mathcal{E}}{\partial y_t} = \frac{\partial \mathcal{E}}{\partial y_L} \cdot \prod_{k=t}^{L-1} g_k \quad (24)$$

This model is easy to optimize because  $\frac{\partial \mathcal{E}}{\partial y_L}$  can be passed to lower-level blocks with no scales. Note that, the methods here are instances of parameter sharing (Dehghani et al., 2019). For example, in each ODE block, we use the same function  $F$  with the same parameter  $\theta_t$  for all intermediate steps. Setting  $\gamma_i = 1$  is a further step towards this because  $F_i$  is passed to next steps with the same scale. Here we call it implicit parameter sharing.

Another method of scaling  $F_i$  is to learn the coefficients automatically on the training data (with the initial value  $\gamma_i = 1$ ). It helps the system learn the way of flowing  $F_i$  in a block. Our experiments show that the automatic coefficient learning is necessary for better results (see Section 4).

Model	Layers	WMT En-De				WMT En-Fr			
		#Param	Steps	BLEU	SBLEU	#Param	Steps	BLEU	SBLEU
Vaswani et al. (2017) - Transformer	6-6	213M	100K	28.40	-	222M	300K	41.00	-
Ott et al. (2018) - Scaling NMT	6-6	210M	100K	29.30	28.6	222M	100K	43.20	41.4
Dehghani et al. (2019) - Universal Transformer	-	-	-	28.90	-	-	-	-	-
Lu et al. (2019) - MacaronNet	6-6	-	-	30.20	-	-	-	-	-
Fan et al. (2020) - LayerDrop	12-6	286M	100K	30.20	-	-	-	-	-
Wu et al. (2019) - Depth growing	8-8	270M	800K	29.92	-	-	-	43.27	-
Wang et al. (2019) - Transformer-DLCL	30-6	137M	50K	29.30	28.6	-	-	-	-
Zhang et al. (2019) - Depth-wise Scale	20-20	560M	300K	29.62	29.0	108M	300K	40.58	-
Wei et al. (2020) - Multiscale Collaborative	18-6	512M	300K	30.56	-	-	-	-	-
Liu et al. (2020) - ADMIN	60-12	262M	250K	30.01	29.5	-	250K	43.80	41.8
Li et al. (2020) - SDT	48-6	192M	50K	30.21	29.0	198M	100K	43.28	41.5
Zhu et al. (2020) - BERT-fused model	6-6	-	-	30.71	-	-	-	43.78	-
<b>Base and Deep Models</b>									
Residual-block	6-6	61M	50K	27.89	26.8	69M	100K	41.05	39.1
RK2-block (learnable $\gamma_i$ )	6-6	61M	50K	28.86	27.7	69M	100K	42.31	40.3
RK4-block	6-6	61M	50K	29.03	27.9	69M	100K	42.56	40.6
Residual-block	24-6	118M	50K	29.43	28.3	123M	100K	42.67	40.6
RK2-block (learnable $\gamma_i$ )	24-6	118M	50K	<b>30.29</b>	<b>29.2</b>	123M	100K	<b>43.48</b>	<b>41.5</b>
RK4-block	24-6	118M	50K	29.80	28.8	123M	100K	43.28	41.3
<b>Wide Models</b>									
Residual-block-Big	6-6	211M	100K	29.21	28.1	221M	100K	42.89	40.9
RK2-block (learnable $\gamma_i$ )	6-6	211M	100K	30.53	29.4	221M	100K	43.59	41.6
Residual-block-Big	12-6	286M	100K	29.91	28.9	297M	100K	43.22	41.2
RK2-block (learnable $\gamma_i$ )	12-6	286M	100K	<b>30.76</b>	<b>29.6</b>	297M	100K	<b>44.11</b>	<b>42.2</b>

Table 1: Comparison with the state-of-the-arts on WMT En-De and WMT En-Fr tasks. We both report the tokenized BLEU and sacrebleu scores for comparison with previous work.

## 4 Experiments

### 4.1 Experimental Setups

Our proposed methods were evaluated on three widely-used benchmarks: the WMT’14 English-German (En-De), WMT’14 English-French (En-Fr) and WMT’16 English-Romanian (En-Ro) translation tasks.

**Datasets and Evaluations:** For the En-De task, the training data consisted of approximately 4.5M tokenized sentence pairs, as in (Vaswani et al., 2017). All sentences were segmented into sequences of sub-word units (Sennrich et al., 2016) with 32K merge operations using a shared vocabulary. We selected *newstest2013* as the validation data and *newstest2014* as the test data. For the En-Fr task, we used the dataset provided by Fairseq, i.e., 36M training sentence pairs from WMT’14. *newstest2012+newstest2013* was the validation data and *newstest2014* was the test data. For the En-Ro task, we replicated the setup of (Mehta et al., 2020), which used 600K/2K/2K sentence pairs for training, evaluation and inference, respectively.

We measured performance in terms of BLEU

(Papineni et al., 2002). Both tokenized BLEU scores<sup>5</sup> and sacrebleu<sup>6</sup> were reported on the En-De and the En-Fr tasks. Also, we report tokenized BLEU scores on the En-Ro task. The beam size and length penalty were set to 4 and 0.6 for the En-De and the En-Fr, and 5 and 1.3 for the En-Ro.

**Training Details:** As suggested in Li et al. (2020)’s work, we used relative positional representation (RPR) for a stronger baseline (Shaw et al., 2018). All experiments were trained on 8 GPUs, with 4,096 tokens on each GPU. For the En-De and the En-Fr tasks, we employed the gradient accumulation strategy with a step of 2 and 8, respectively. We used the Adam optimizer (Kingma and Ba, 2015) whose hyperparameters were set to (0.9, 0.997), and the max point of the learning rate was set to 0.002 for fast convergence. We regard merging SAN and FFN as the default ODE block. More details could be found in our supplementary materials.

<sup>5</sup>Computed by *multi-bleu.perl*

<sup>6</sup>BLEU+case.mixed+numrefs.1+smooth.exp+tok.13a+version.1.2.12

Model	Params	Epochs	BLEU
Transformer in Mehta et al. (2020)	62M	170	34.30
DeLight (Mehta et al., 2020)	53M	170	34.70
Int Transformer <sup>†</sup> (Lin et al., 2020)	-	-	32.60
Transformer (Our impl.)	69M	20	33.49
RK2-block (learnable $\gamma_i$ )	69M	20	34.94
RK2-block-Big (learnable $\gamma_i$ )	226M	20	<b>35.28</b>

Table 2: Results on the WMT En-Ro task. <sup>†</sup> indicates the related information is not reported.

## 4.2 Results

**Results of En-De and En-Fr:** Table 1 compares ODE Transformer with several state-of-the-art systems. Both RK2-block and RK4-block outperform the baselines by a large margin with different model capacities. For example, RK2-block obtains a 0.97 BLEU improvement with the base configuration when the depth is 6. RK4-block yields a gain of +0.17 BLEU points on top of RK2-block. This observation empirically validates the conjecture that high-order ODE functions are more efficient. When we switch to deep models, RK2-block is comparable with a 48-layer strong system reported in (Li et al., 2020) with significantly fewer parameters, indicating our method is parameter efficient.

Wide models can also benefit from the enlarging layer depth (Wei et al., 2020; Li et al., 2020). The RK-2 ODE Transformer achieves BLEU score of 30.76 and 44.11 on the En-De and the En-Fr tasks, significantly surpassing the standard Big model by 1.32 and 0.70 BLEU points. This sets a new state-of-the-art on these tasks with fewer parameters. Note that more results on RK4-block (learnable  $\gamma_i$ ) will be reported.

**Results of En-Ro:** Table 2 exhibits model parameters, total training steps and BLEU scores of several strong systems on the En-Ro task. Again, ODE Transformer outperforms these baseline. As stated in (Mehta et al., 2020), they trained the model up to 170 epochs and obtained a BLEU score of 34.70 through the DeLight model. However, the observation here is quite different. The validation perplexity begins to increase after 20 epochs. Thus, our baseline is slightly inferior to theirs, but matches the result reported in Lin et al. (2020). ODE Transformer achieves even better performance with DeLight within much less training cost. For a bigger model (line 6 in Table 2), it obtains a BLEU score of 35.28.

Model	Params	BLEU
Transformer (Vaswani et al., 2017)	62M	27.30
Evolved Transformer (So et al., 2019)	46M	27.70
Lite Transformer <sup>†</sup> (Wu et al., 2020)	-	26.50
DeLight (Mehta et al., 2020)	37M	27.60
RK2-block (learnable $\gamma_i$ )	37M	<b>28.24</b>
RK2-block (learnable $\gamma_i$ )	29M	27.84

Table 3: The comparison of model efficiency on the WMT En-De task.

**Parameter Efficiency:** Table 3 summaries the results of several efficient Transformer variants, including Lite Transformer (Wu et al., 2020), DeLight (Mehta et al., 2020) and a light version of the Evolved Transformer (So et al., 2019). As we expected, the proposed ODE Transformer is promising for smaller models. It is comparable in BLEU with DeLight but having 9M fewer parameters. Under the same model capacity, it outperforms DeLight by 0.84 BLEU points. These results demonstrate that the proposed method is orthogonal to the model capacity. It may offer a new choice for deploying NMT systems on edge devices.

## 4.3 Analysis

Here we investigate some interesting issues. For simplicity, in the following, we call RK2-block with learnable coefficients as RK2-block-v2.

**BLEU against Encoder Depth:** Figure 3 (left) depicts BLEU scores of several ODE Transformer variants and the baseline under different encoder depths. All ODE Transformer variants are significantly superior to the baseline when the depth  $\leq 24$ . And the RK2-block-v2 almost achieves the best performance over all depths, especially when the model becomes deeper. Intuitively, a 6-layer RK2-block is able to deliver comparable performance compared with the 18-layer baseline system. Again, it indicates the proposed method is parameter efficient. Another finding here is RK4-block behaves strong on shallow models, similar phenomena are observed in Table 1. It is inferior to RK2-block for deeper models, though high-order ODE solvers can obtain lower errors. This is due to original coefficients may cause the optimization problem in the backward propagation when the model is deep (see Section 3.2). Also, Figure 3 (right) plots BLEU as a function of the model size when the hidden size is 256. Our RK2 method significantly surpasses the baseline using much fewer parameters.

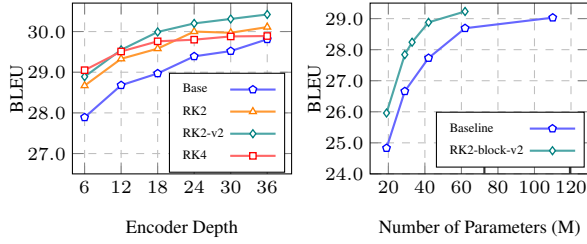


Figure 3: The comparison of BLEU against different encoder depth and the number of model parameters.

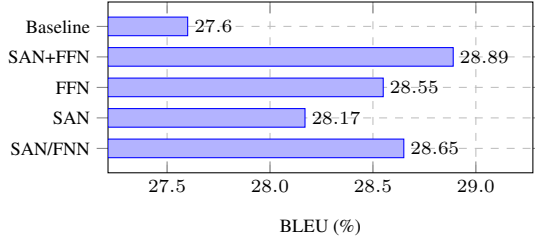


Figure 4: BLEU scores [%] of several  $F(\cdot, \cdot)$  on the WMT En-De task.

**Ablation Study on Different  $F(\cdot, \cdot)$ :** As we stated, the  $F(\cdot, \cdot)$  function can either be the sub-layer, e.g. SAN, FFN or both of them (SAN+FFN). As shown in Figure 4, high-order ODE works better with FFN than SAN. An exploration might be that the FFN component has more parameters than the SAN component<sup>7</sup>. The model that merging FFN and SAN as an ODE block shows the best performance.

**Training and Validation Perplexity:** Figure 5 plots the training and validation perplexity (PPL) curves of RK blocks and the standard residual-block. We compare the behaviors based on two configurations (base and wide models). Intuitively, RK2-block presents lower training and validation PPLs in both configurations.

**Visualization of the Gradient Norm:** To study the superiority of the proposed ODE Transformer, we collect the gradient norm of several well-trained systems during training. Figure 6 plots the gradient norm of RK2-block, RK4-block and the standard residual-block (baseline). As we can see that Pre-Norm residual block is able to make the training stable (Wang et al., 2019). Both RK2-block and RK4-block provide richer signals due to the implicit parameter sharing among intermediate approximations. And the two learning curves likewise appear to be nearly the same, which is consistent

<sup>7</sup>Mostly, there are  $2 \cdot d_{\text{model}} \cdot 4d_{\text{model}}$  parameters in FFN and  $d_{\text{model}} \cdot 3d_{\text{model}} + d_{\text{model}} \cdot d_{\text{model}}$  in SAN.

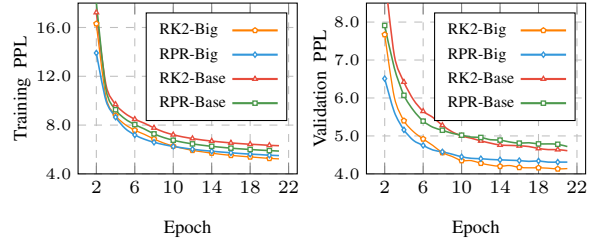


Figure 5: The comparison of training and validation PPL on base and wide models.

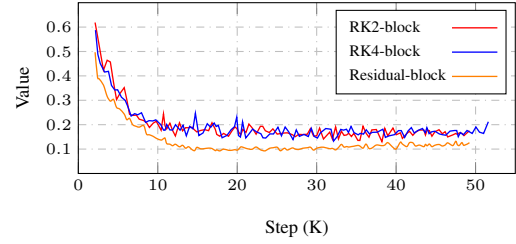


Figure 6: Visualization of the gradient norm of ODE Transformers compared with the baseline.

with the result in Table 1.

### Comparison of Different ODE Design Schemas:

Then, we take a comprehensive analysis of several ODE design schemas. As stated in Lu et al. (2018), several models in computer vision, such as LeapfrogNet (He et al., 2019), PolyNet (Zhang et al., 2017), Multi-step Net (Lu et al., 2018) can also be interpreted from the ODE perspective. The related ODE functions are summarized in Table 4. Here, we re-implement these methods using the same codebase for fair comparisons. We set the encoder depth as 6 following the base configuration and conducted experiments on the En-De task.

At time  $t$ , Multistep Euler methods requires previous states, e.g.  $y_{t-1}$ , to generate the current approximation, instead of iterative refinements based on the current-time state. Basically, these methods are not parameter efficient, and obtain inferior performance than ours. Note that DLCL can also be regarded as a multistep Euler method, which is more competitive in deep Transformer. But there is only a small improvement upon a shallow baseline. Theoretically, the Backward Euler method is slightly better than the Forward Euler method in numerical analysis, but the improvement is marginal. Note that our ODE Transformer achieves consistent BLEU improvements over the aforementioned methods. The reason here is that this kind of iterative refinements enable the parameters learning more efficient and effective. All models could be

Model	Information Flow	Related ODEs	BLEU
He et al. (2019) - Leapfrog	$y_{t+1} = y_{t-1} + 2F(y_t, \theta_t)$	Multistep Euler	28.07
Lu et al. (2018) - Multistep	$y_{t+1} = k_n \cdot y_t + (1 - k_n) \cdot y_{t-1} + F(y_t, \theta_t)$	Multistep Euler	28.17
Wang et al. (2019) - DLCL	$y_{t+1} = y_0 + \sum_{i=0}^t W_i F(y_i, \theta_i)$	Multistep Euler	27.78
Zhang et al. (2017) - PolyNet	$y_{t+1} = y_t + F(y_t, \theta_t) + F(F(y_t, \theta_t), \theta_t)$	Backward Euler	28.15
RK2-block	$y_{t+1} = y_t + \frac{1}{2}F(y_t, \theta_t) + \frac{1}{2}F(y_t + F(y_t, \theta_t), \theta_t)$	Improved Euler	28.57
RK2-block ( $\gamma_i = 1$ )	$y_{t+1} = y_t + F(y_t, \theta_t) + F(y_t + F(y_t, \theta_t), \theta_t)$	Runge-Kutta 2nd-order	28.77
RK2-block (learnable $\gamma_i$ )	$y_{t+1} = y_t + \gamma_1 \cdot F(y_t, \theta_t) + \gamma_2 \cdot F(y_t + F(y_t, \theta_t), \theta_t)$	Runge-Kutta 2nd-order	28.86
RK4-block	$y_{t+1} = y_t + \frac{1}{6}F_1 + \frac{2}{6}F_2 + \frac{2}{6}F_3 + \frac{1}{6}F_4$	Runge-Kutta 4th-order	29.03

Table 4: Comparison of several ODE-inspired design schemas on the En-De task. We re-implement and apply these methods into Transformer. Note that  $y_n$  denotes the model input of layer n. Due to the limited space, we use  $F_i$  to denote the intermediate representation, where  $i \in [1, 4]$ .

Model	1-layer PPL	2-layer PPL
Residual Block	142.33	136.07
RK2-block	131.80	123.12
RK2-block ( $\gamma_i = 1$ )	132.67	123.90
RK2-block (learnable $\gamma_i$ )	128.48	121.02
RK4-block	<b>126.89</b>	<b>119.46</b>

Table 5: The comparison of PPL on several systems. More details refer to the supplementary materials.

found in our attachment.

**Quantization of the Truncation Error:** Here, we aim at quantifying the truncation error. However, we cannot obtain the “true” solution of each block output in NMT, because we mainly experimented on the encoder side. Instead, we experimented on the language modeling task, where the loss between a single layer model output and the ground truth is equivalent to the truncation error without error propagations. Table 5 shows the PPL on the PTB task. All ODE Transformer variants reduce the errors significantly. RK4-order achieves the lowest PPL on both settings. In addition, a RK2-block can even obtain lower PPL than a 2-layer residual-block. The observation here again verifies our conjecture.

## 5 Related Work

**Deep Transformer models:** Recently, deep Transformer has witnessed tremendous success in machine translation. A straightforward way is to shorten the path from upper-level layers to lower-level layers thus to alleviate the gradient vanishing or exploding problems (Bapna et al., 2018; Wang et al., 2019; Wu et al., 2019; Wei et al., 2020). For deeper models, the training cost is nonnegligible. To speed up the training, an alternative way is to train a shallow model first and progressively in-

creasing the model depth (Li et al., 2020; Dong et al., 2020).

Apart from the model architecture improvements, another way of easing the optimization is to utilize carefully designed parameter initialization strategies, such as depth-scale (Zhang et al., 2019), Lipschitz constraint (Xu et al., 2020), T-fixup (Huang et al., 2020) and ADMIN (Liu et al., 2020). Note that the ODE Transformer is orthogonal to the aforementioned methods, and we will test it on these methods in the future work.

**Ordinary Differential Equations:** The relationship between the ResNet and ODEs was first proposed by Weinan (2017). This brings the community a brand-new perspective on the design of effective deep architectures. Some insightful architectures (Zhang et al., 2017; Larsson et al., 2017; Lu et al., 2018; He et al., 2019) can also be interpreted from the ODE perspective. But, in nature language processing, it is still rare to see studies on designing models from the ODE perspective. Perhaps the most relevant work with us is Lu et al. (2019)’s work. They interpreted the Transformer architecture from a multi-particle dynamic system view and relocated the self-attention sandwiched into the FFN. Unlike their work, we argue that the stacked first-order ODE blocks may cause error accumulation, thus hindering the model performance. We address this issue by introducing high-order blocks, and demonstrate significant BLEU improvements.

## 6 Conclusions

In this paper, we have explored the relationship between Transformer and ODEs. We have proposed a new architecture (ODE Transformer) to help the model benefit from high-order ODE solutions. Ex-



perimental results show that ODE Transformer can significantly outperform the baseline with the same model capacity. It achieves 30.76 and 44.11 BLEU scores on the WMT’14 En-De and En-Fr test data. This sets a new state-of-the-art on the En-Fr task.

## References

- Uri M Ascher and Linda R Petzold. 1998. *Computer methods for ordinary differential equations and differential-algebraic equations*, volume 61. Siam.
- Ankur Bapna, Mia Chen, Orhan Firat, Yuan Cao, and Yonghui Wu. 2018. [Training deeper neural machine translation models with transparent attention](#). In *Proceedings of the 2018 Conference on Empirical Methods in Natural Language Processing*, pages 3028–3033, Brussels, Belgium. Association for Computational Linguistics.
- John C Butcher. 1963. Coefficients for the study of runge-kutta integration processes. *Journal of the Australian Mathematical Society*, 3(2):185–201.
- John Charles Butcher. 1996. A history of runge-kutta methods. *Applied numerical mathematics*, 20(3):247–260.
- Bo Chang, Lili Meng, Eldad Haber, Lars Ruthotto, David Begert, and Elliot Holtham. 2018. Reversible architectures for arbitrarily deep residual neural networks. In *Proceedings of the Thirty-Second AAAI Conference on Artificial Intelligence, (AAAI-18), the 30th innovative Applications of Artificial Intelligence (IAAI-18), and the 8th AAAI Symposium on Educational Advances in Artificial Intelligence (EAAI-18), New Orleans, Louisiana, USA, February 2-7, 2018*, pages 2811–2818. AAAI Press.
- Ricky TQ Chen, Yulia Rubanova, Jesse Bettencourt, and David K Duvenaud. 2018. Neural ordinary differential equations. In *Advances in neural information processing systems*, pages 6571–6583.
- Zihang Dai, Zhilin Yang, Yiming Yang, Jaime Carbonell, Quoc Le, and Ruslan Salakhutdinov. 2019. Transformer-XL: Attentive language models beyond a fixed-length context. In *Proceedings of the 57th Annual Meeting of the Association for Computational Linguistics*, pages 2978–2988, Florence, Italy. Association for Computational Linguistics.
- Mostafa Dehghani, Stephan Gouws, Oriol Vinyals, Jakob Uszkoreit, and Lukasz Kaiser. 2019. Universal transformers. In *7th International Conference on Learning Representations, ICLR 2019, New Orleans, LA, USA, May 6-9, 2019*. OpenReview.net.
- Chengyu Dong, Liyuan Liu, Zichao Li, and Jingbo Shang. 2020. Towards adaptive residual network training: A neural-ode perspective. In *Proceedings of the 37th International Conference on Machine Learning, ICML 2020, 13-18 July 2020, Virtual Event*, volume 119 of *Proceedings of Machine Learning Research*, pages 2616–2626. PMLR.
- Angela Fan, Edouard Grave, and Armand Joulin. 2020. Reducing transformer depth on demand with structured dropout. In *8th International Conference on Learning Representations, ICLR 2020, Addis Ababa, Ethiopia, April 26-30, 2020*. OpenReview.net.
- Klaus Greff, Rupesh Kumar Srivastava, and Jürgen Schmidhuber. 2017. Highway and residual networks learn unrolled iterative estimation. In *5th International Conference on Learning Representations, ICLR 2017, Toulon, France, April 24-26, 2017, Conference Track Proceedings*.
- Eldad Haber and Lars Ruthotto. 2017. Stable architectures for deep neural networks. *Inverse Problems*, 34(1):014004.
- Eldad Haber, Lars Ruthotto, Elliot Holtham, and Seong-Hwan Jun. 2018. Learning across scales - multiscale methods for convolution neural networks. In *Proceedings of the Thirty-Second AAAI Conference on Artificial Intelligence, (AAAI-18), the 30th innovative Applications of Artificial Intelligence (IAAI-18), and the 8th AAAI Symposium on Educational Advances in Artificial Intelligence (EAAI-18), New Orleans, Louisiana, USA, February 2-7, 2018*, pages 3142–3148. AAAI Press.
- Kaiming He, Xiangyu Zhang, Shaoqing Ren, and Jian Sun. 2016. Deep residual learning for image recognition. In *Proceedings of the IEEE conference on computer vision and pattern recognition*, pages 770–778.
- Xiangyu He, Zitao Mo, Peisong Wang, Yang Liu, Mingyuan Yang, and Jian Cheng. 2019. Ode-inspired network design for single image super-resolution. In *IEEE Conference on Computer Vision and Pattern Recognition, CVPR 2019, Long Beach, CA, USA, June 16-20, 2019*, pages 1732–1741. Computer Vision Foundation / IEEE.
- Xiao Shi Huang, Felipe Perez, Jimmy Ba, and Maksims Volkovs. 2020. Improving transformer optimization through better initialization. In *Proceedings of Machine Learning and Systems 2020*, pages 9868–9876.
- Diederik P. Kingma and Jimmy Ba. 2015. Adam: A method for stochastic optimization. In *3rd International Conference on Learning Representations, ICLR 2015, San Diego, CA, USA, May 7-9, 2015, Conference Track Proceedings*.
- Wilhelm Kutta. 1901. Beitrag zur naherungsweise integration totaler differentialgleichungen. *Z. Math. Phys.*, 46:435–453.
- Gustav Larsson, Michael Maire, and Gregory Shakhnarovich. 2017. Fractalnet: Ultra-deep neural networks without residuals. In *5th International Conference on Learning Representations, ICLR 2017, Toulon, France, April 24-26, 2017, Conference Track Proceedings*. OpenReview.net.

- Bei Li, Ziyang Wang, Hui Liu, Yufan Jiang, Quan Du, Tong Xiao, Huizhen Wang, and Jingbo Zhu. 2020. Shallow-to-deep training for neural machine translation. In *Proceedings of the 2020 Conference on Empirical Methods in Natural Language Processing (EMNLP)*, pages 995–1005, Online. Association for Computational Linguistics.
- Ye Lin, Yanyang Li, Tengbo Liu, Tong Xiao, Tongran Liu, and Jingbo Zhu. 2020. Towards fully 8-bit integer inference for the transformer model. In *Proceedings of the Twenty-Ninth International Joint Conference on Artificial Intelligence, IJCAI 2020*, pages 3759–3765. ijcai.org.
- Liyuan Liu, Xiaodong Liu, Jianfeng Gao, Weizhu Chen, and Jiawei Han. 2020. [Understanding the difficulty of training transformers](#). In *Proceedings of the 2020 Conference on Empirical Methods in Natural Language Processing (EMNLP)*, pages 5747–5763, Online. Association for Computational Linguistics.
- Yiping Lu, Zhuohan Li, Di He, Zhiqing Sun, Bin Dong, Tao Qin, Liwei Wang, and Tie-Yan Liu. 2019. Understanding and improving transformer from a multi-particle dynamic system point of view. *arXiv preprint arXiv:1906.02762*.
- Yiping Lu, Aoxiao Zhong, Quanzheng Li, and Bin Dong. 2018. Beyond finite layer neural networks: Bridging deep architectures and numerical differential equations. In *Proceedings of the 35th International Conference on Machine Learning, ICML 2018, Stockholmsmässan, Stockholm, Sweden, July 10-15, 2018*, pages 3282–3291.
- Sachin Mehta, Marjan Ghazvininejad, Srinivasan Iyer, Luke Zettlemoyer, and Hannaneh Hajishirzi. 2020. Delight: Very deep and light-weight transformer. *arXiv preprint arXiv:2008.00623*.
- Myle Ott, Sergey Edunov, David Grangier, and Michael Auli. 2018. [Scaling neural machine translation](#). In *Proceedings of the Third Conference on Machine Translation, Volume 1: Research Papers*, pages 1–9, Belgium, Brussels. Association for Computational Linguistics.
- Kishore Papineni, Salim Roukos, Todd Ward, and Wei-Jing Zhu. 2002. [Bleu: a method for automatic evaluation of machine translation](#). In *Proceedings of the 40th Annual Meeting of the Association for Computational Linguistics*, pages 311–318, Philadelphia, Pennsylvania, USA. Association for Computational Linguistics.
- Carl Runge. 1895. Über die numerische auflösung von differentialgleichungen. *Mathematische Annalen*, 46(2):167–178.
- Lars Ruthotto and Eldad Haber. 2019. Deep neural networks motivated by partial differential equations. *Journal of Mathematical Imaging and Vision* volume, 62:352–364.
- Rico Sennrich, Barry Haddow, and Alexandra Birch. 2016. [Neural machine translation of rare words with subword units](#). In *Proceedings of the 54th Annual Meeting of the Association for Computational Linguistics (Volume 1: Long Papers)*, pages 1715–1725, Berlin, Germany. Association for Computational Linguistics.
- Peter Shaw, Jakob Uszkoreit, and Ashish Vaswani. 2018. [Self-attention with relative position representations](#). In *Proceedings of the 2018 Conference of the North American Chapter of the Association for Computational Linguistics: Human Language Technologies, Volume 2 (Short Papers)*, pages 464–468, New Orleans, Louisiana. Association for Computational Linguistics.
- David R. So, Quoc V. Le, and Chen Liang. 2019. The evolved transformer. In *Proceedings of the 36th International Conference on Machine Learning, ICML 2019, 9-15 June 2019, Long Beach, California, USA*, volume 97 of *Proceedings of Machine Learning Research*, pages 5877–5886. PMLR.
- Ashish Vaswani, Noam Shazeer, Niki Parmar, Jakob Uszkoreit, Llion Jones, Aidan N Gomez, Łukasz Kaiser, and Illia Polosukhin. 2017. Attention is all you need. In *Advances in Neural Information Processing Systems*, pages 6000–6010.
- Qiang Wang, Bei Li, Tong Xiao, Jingbo Zhu, Changliang Li, Derek F. Wong, and Lidia S. Chao. 2019. [Learning deep transformer models for machine translation](#). In *Proceedings of the 57th Annual Meeting of the Association for Computational Linguistics*, pages 1810–1822, Florence, Italy. Association for Computational Linguistics.
- Xiangpeng Wei, Heng Yu, Yue Hu, Yue Zhang, Rongxiang Weng, and Weihua Luo. 2020. [Multiscale collaborative deep models for neural machine translation](#). In *Proceedings of the 58th Annual Meeting of the Association for Computational Linguistics*, pages 414–426, Online. Association for Computational Linguistics.
- E Weinan. 2017. A proposal on machine learning via dynamical systems. *Communications in Mathematics and Statistics*, 5(1):1–11.
- Lijun Wu, Yiren Wang, Yingce Xia, Fei Tian, Fei Gao, Tao Qin, Jianhuang Lai, and Tie-Yan Liu. 2019. Depth growing for neural machine translation. In *Proceedings of the 57th Annual Meeting of the Association for Computational Linguistics*, pages 5558–5563, Florence, Italy.
- Zhanghao Wu, Zhijian Liu, Ji Lin, Yujun Lin, and Song Han. 2020. Lite transformer with long-short range attention. In *8th International Conference on Learning Representations, ICLR 2020, Addis Ababa, Ethiopia, April 26-30, 2020*. OpenReview.net.
- Hongfei Xu, Qiuhui Liu, Josef van Genabith, Deyi Xiong, and Jingyi Zhang. 2020. [Lipschitz constrained parameter initialization for deep transformers](#). In *Proceedings of the 58th Annual Meeting*

of the Association for Computational Linguistics, pages 397–402, Online. Association for Computational Linguistics.

Biao Zhang, Ivan Titov, and Rico Sennrich. 2019. Improving deep transformer with depth-scaled initialization and merged attention. In *Proceedings of the 2019 Conference on Empirical Methods in Natural Language Processing and the 9th International Joint Conference on Natural Language Processing (EMNLP-IJCNLP)*, pages 898–909, Hong Kong, China. Association for Computational Linguistics.

Xingcheng Zhang, Zhizhong Li, Chen Change Loy, and Dahua Lin. 2017. Polynet: A pursuit of structural diversity in very deep networks. In *2017 IEEE Conference on Computer Vision and Pattern Recognition, CVPR 2017, Honolulu, HI, USA, July 21-26, 2017*, pages 3900–3908. IEEE Computer Society.

Jinhua Zhu, Yingce Xia, Lijun Wu, Di He, Tao Qin, Wengang Zhou, Houqiang Li, and Tie-Yan Liu. 2020. Incorporating BERT into neural machine translation. In *8th International Conference on Learning Representations, ICLR 2020, Addis Ababa, Ethiopia, April 26-30, 2020*. OpenReview.net.

## A Details for Experimental Steps and Datasets

All models were trained on 8 NVIDIA TITAN V GPUs with mix-precision accelerating. And main results were the average of three times running with different random seeds. Note that we averaged the last 5/10 checkpoints for more robust results.

Since the proposed method is orthogonal to the model capacity, we evaluated the ODE Transformer on Base/Deep/Wide configurations, respectively. The detail of each configuration is as follows:

- **Base/Deep Model.** The hidden size of self-attention was 512, and the dimension of the inner-layer in FFN was 2,048. We used 8 heads for attention. For training, we set all dropout to 0.1, including residual dropout, attention dropout, ReLU dropout. Label smoothing  $\epsilon_{ls} = 0.1$  was applied to enhance the generation ability of the model. For deep models, we only enlarged the encoder depth considering the inference speed.
- **Wide (or Big) Model.** We used the same architecture as Transformer-Base but with a larger hidden layer size 1,024, more attention heads (16), and a larger feed forward inner-layer (4,096 dimensions). The residual dropout was set to 0.3 for the En-De task and 0.1 for the En-Fr tasks.

Lang	Train	Valid	Test
WMT’14 En-De	4.5M	3000	3003
WMT’14 En-Fr	35.7M	26822	3003
WMT’16 En-Ro	602K	1999	1999

Table 6: The comparison of PPL on several systems.

In the training phase, Deep/Big models were updated for 50K and 100K steps on the En-De task, 100K steps on the En-Fr task, 17K steps on the En-Ro task.

Table 6 summarizes the details of our datasets, including the WMT En-De, the WMT En-Fr and the WMT En-Ro tasks. We both present the sentences and tokens of each task. For En-De and En-Fr task, the datasets used in this work could be found in Fairseq<sup>8</sup>. For En-Ro, one can use the preprocessed dataset provided by DeLight<sup>9</sup>. Note that we only share the target embedding and the softmax embedding instead of a shared vocabulary between the source side and the target side.

## B Details for the PTB dataset

Here, we introduce the details about the PTB dataset and the corresponding configuration. It contains 88K, 3370 and 3761 sentences for training, validation and test. The vocabulary size was 10K. In this work, the layer depth of the language model was set to 1 or 2. The main concern here is to evaluate the truncate error. Assume the layer depth is 1, then the loss between the block output and the ground-truth can be regarded as the truncate error. It alleviates the influence of the error accumulation among different layers.

The hidden size was 512, and the filter size of the FFN was 2,048. We set all the dropout rate as 0.1, including the residual dropout, attention dropout and the relu dropout. Each model was trained up to 20 epochs, and most models achieved the lowest PPL on the validation set when the epoch is 10. Then the validation PPL began to increase, though the training PPL is still declining. The warmup-step was 2000 and the batch size was 4,096. The max learning rate was set to 0.0007. After warmup, the learning rate decayed proportionally to the inverse square root of the current step.

<sup>8</sup>[https://github.com/pytorch/fairseq/tree/master/examples/scaling\\_nmt](https://github.com/pytorch/fairseq/tree/master/examples/scaling_nmt)

<sup>9</sup>[https://github.com/sacmehta/delight/blob/master/readme\\_files/nmt/wmt16\\_en2ro.md](https://github.com/sacmehta/delight/blob/master/readme_files/nmt/wmt16_en2ro.md)

## C Derivations of the Equation

Let  $\mathcal{E}$  be the loss of training,  $L$  be the number blocks of the model, and  $y_L$  be the model output. Here, we define

$$z_k = y_k + F(y_k, \theta_k) \quad (25)$$

Then the information flow of the RK2 method can be described as follows:

$$\begin{aligned} y_{k+1} &= y_k + \frac{1}{2}F(y_k, \theta_k) + \\ &\quad \frac{1}{2}F(y_k + F(y_k, \theta_k), \theta_k) \\ &= y_k + \frac{1}{2}F(y_k, \theta_k) + \frac{1}{2}F(z_k, \theta_k) \end{aligned} \quad (26)$$

where  $\frac{\partial z_k}{\partial y_k} = 1 + \frac{\partial F(y_k, \theta_k)}{\partial y_k}$ . In this way, the detail derivation of Eq. (26) is as follows:

$$\begin{aligned} \frac{\partial y_{k+1}}{\partial y_k} &= 1 + \frac{1}{2} \frac{\partial F(y_k, \theta_k)}{\partial y_k} + \frac{1}{2} \frac{\partial F(z_k, \theta_k)}{\partial z_k} \cdot \frac{\partial z_k}{\partial y_k} \\ &= \frac{1}{2} \cdot \left( 1 + 1 + \frac{\partial F(y_k, \theta_k)}{\partial y_k} + \frac{\partial F(z_k, \theta_k)}{\partial z_k} \cdot \left( 1 + \frac{\partial F(y_k, \theta_k)}{\partial y_k} \right) \right) \\ &= \frac{1}{2} \cdot \left( 1 + \left( 1 + \frac{\partial F(z_k, \theta_k)}{\partial z_k} \right) \cdot \left( 1 + \frac{\partial F(y_k, \theta_k)}{\partial y_k} \right) \right) \end{aligned} \quad (27)$$

With the chain rule, the error  $\mathcal{E}$  propagates from the top layer  $y_L$  to layer  $y_t$  by the following formula:

$$\frac{\partial \mathcal{E}}{\partial y_t} = \frac{\partial \mathcal{E}}{\partial y_L} \cdot \frac{\partial y_L}{\partial y_{L-1}} \cdot \frac{\partial y_{L-1}}{\partial y_{L-2}} \cdots \frac{\partial y_{t+1}}{\partial y_t}$$

Here we have

$$g_k = \left( 1 + \frac{\partial F(y_k, \theta_k)}{\partial y_k} \right) \cdot \left( 1 + \frac{\partial F(z_k, \theta_k)}{\partial z_k} \right) \quad (28)$$

Then, put the Eq. (28) into Eq. (27), the gradient of  $\mathcal{E}$  at  $y_t$  is

$$\frac{\partial \mathcal{E}}{\partial y_t} = \frac{\partial \mathcal{E}}{\partial y_L} \cdot \frac{1}{2^{L-t}} \cdot \prod_{k=t}^{L-1} (1 + g_k) \quad (29)$$

Similarly, we can easily obtain the gradient of RK2 method where  $\gamma_i = 1$ :

$$\begin{aligned} \frac{\partial \mathcal{E}}{\partial y_t} &= \frac{\partial \mathcal{E}}{\partial y_L} \cdot g_{L-1} \cdot g_{L-2} \cdots g_t \\ &= \frac{\partial \mathcal{E}}{\partial y_L} \cdot \prod_{k=t}^{L-1} g_k \end{aligned} \quad (30)$$